Molecular Bases of Disease:

Quantitative Mapping of Reversible Mitochondrial Complex I Cysteine Oxidation in a Parkinson Disease Mouse Model

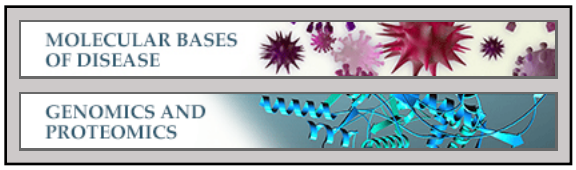

Steven R. Danielson, Jason M. Held, May Oo, Rebeccah Riley, Bradford W. Gibson and Julie K. Andersen

J. Biol. Chem. 2011, 286:7601-7608.
doi: 10.1074/jbc.M110.190108 originally published online January 1, 2011

THE JOURNAL OF BIOLOGICAL CHEMISTRY VOL. 286, NO. 9, pp. 7601–7608, March 4, 2011

Quantitative Mapping of Reversible Mitochondrial Complex I Cysteine Oxidation in a Parkinson Disease Mouse Model*[S]

Received for publication, September 29, 2010, and in revised form, December 15, 2010 Published, JBC Papers in Press, January 1, 2011, DOI 10.1074/jbc.M110.190108

Steven R. Danielson, Jason M. Held, May Oo, Rebeccah Riley, Bradford W. Gibson[1], and Julie K. Andersen[2]

From the Buck Institute for Age Research, Novato, California 94945

Differential cysteine oxidation within mitochondrial Complex I has been quantified in an *in vivo* oxidative stress model of Parkinson disease. We developed a strategy that incorporates rapid and efficient immunoaffinity purification of Complex I followed by differential alkylation and quantitative detection using sensitive mass spectrometry techniques. This method allowed us to quantify the reversible cysteine oxidation status of 34 distinct cysteine residues out of a total 130 present in murine Complex I. Six Complex I cysteine residues were found to display an increase in oxidation relative to controls in brains from mice undergoing *in vivo* glutathione depletion. Three of these residues were found to reside within iron-sulfur clusters of Complex I, suggesting that their redox state may affect electron transport function.

Mitochondrial Complex I is a transmembrane protein complex composed of at least 45 subunits which is the first and largest (~1 MDa) of the electron transport chain complexes, where it plays a central function in aerobic respiration. The relationship between Parkinson disease (PD)[3] and Complex I inhibition has been extensively studied since the discovery that treatment with 1-methyl-4-phenyl-1,2,3,6-tetrahydropyridine (MPTP) and rotenone, Complex I-specific inhibitors, results in PD-like neuropathology (1, 2). Subsequently, Complex I deficiency has been noted in postmortem substantia nigra samples from PD patients, the brain region preferentially impacted by the disease further linking PD and reduced Complex I activity (3). The cause of the selective Complex I inhibition in PD is, however, unknown.

Total glutathione (GSH+GSSG) depletion is the earliest known indication of oxidative stress in PD, occurring prior to decreases in mitochondrial Complex I activity and dopamine levels (4–6). Previously, our laboratory demonstrated that total glutathione levels within murine nigrostriatal tissues can be decreased by 40–50% via intraperitoneal injection of the glutathione synthesis inhibitor L-buthionine (*S,R*)-sulfoximine (BSO), replicating biochemical conditions observed in the Parkinsonian brain (7). Decreased glutathione levels were subsequently found to result in selective inhibition of Complex I activity both *in vitro* and *in vivo*. Selective reductions in Complex I activity could be returned to normal levels by restoration of glutathione levels or by the addition of the sulfhydryl-reducing agent dithiothreitol (DTT), suggesting that inhibition may be due to reversible oxidation of cysteine residues within one or more key subunits (8–12).

Relative to other amino acids, cysteine residues are among the most sensitive to oxidation, and alterations in the redox state of cysteine residues can alter protein structure and enzyme activity (13, 14). Cysteine oxidation can result in a diverse array of modifications including some that have been demonstrated to be reversible *in vivo* through interactions with glutathione or thioredoxin or *in vitro* via treatment with mild chemical reducing reagents such as DTT. Reversible cysteine oxidative modifications include intramolecular disulfides, *S*-nitrosylation, *S*-glutathionylation, and sulfenic acid (SOH), whereas irreversible cysteine oxidative modifications include sulfinic (SO_2H) and sulfonic acid (SO_3H) (14, 15).

Evidence of oxidative cysteine modifications within mitochondrial Complex I have been described previously (16, 17). However, systematic mapping and quantitation of reversible cysteine oxidations within the subunits that make up this complex have not been reported. We have recently developed and validated a sensitive method for identifying and quantifying multiple cysteine oxidation events at low (attomole) levels (18). In this current study, we have adapted this technique to map the reversible oxidation status of ~26% of the total cysteine residues within Complex I isolated from control *versus* glutathione-depleted mouse brains.

EXPERIMENTAL PROCEDURES

Animals—Protocols for animal experiments described in this study were performed in accordance with National Institutes of Health guidelines and approved by the Institutional Animal Care and Use Committee (IACUC) at the Buck Institute. Young adult (7 weeks old) male mice (C57BL/6J) were obtained from Jackson Laboratory (Bar Harbor, ME). Mice were acclimated to our vivarium for 2 weeks before initiation of experiments. Mice had free access to food and water and were maintained on a 12-h light/dark cycle.

* This work was supported, in whole or in part, by National Institutes of Health Grants P01 AG025901 (to J. K. A.), PL1 AG032118 (to B. W. G.), S10 RR024615 (to B. W. G.), and S10 RR0021222 (to B. W. G.). This work was also supported by a grant from the W. M. Keck Foundation (to J. K. A. and B. W. G.).

[S] The on-line version of this article (available at http://www.jbc.org) contains supplemental Tables 1–4 and Figs. 1–44.

[1] To whom correspondence may be addressed: Buck Institute for Age Research, 8001 Redwood Blvd., Novato, CA 94945. Tel.: 415-209-2000; Fax: 415-209-2231; E-mail: bgibson@buckinstitute.org.

[2] To whom correspondence may be addressed: Buck Institute for Age Research, 8001 Redwood Blvd., Novato, CA 94945. Tel.: 415-209-2000; Fax: 415-209-2231; E-mail: jandersen@buckinstitute.org.

[3] The abbreviations used are: PD, Parkinson disease; BisTris, bis(2-hydroxyethyl)iminotris(hydroxymethyl)methane; BSO, L-buthionine (*S,R*)-sulfoximine; EPI, enhanced product ion; MRM, multiple reaction monitoring; MS/MS, tandem MS; NEM, *N*-ethylmaleimide; SOH, sulfenic acid; Tricine, *N*-[2-hydroxy-1,1-bis(hydroxymethyl)ethyl]glycine.

Drug Administration and Tissue Isolation—BSO was dissolved in sterile saline solution and injected intraperitoneally at a dose of 3 mmol/kg body weight according to our previously published protocol. Control mice received an equal volume of sterile saline solution. Treated and control mice received three total injections, once a day for 3 days. Mice were killed 24 h following the final injection, and whole brains were isolated as described previously (7); $n = 6$ (3 control, 3 BSO-treated).

Complex I Isolation, Stepwise Alkylation, and Digestion—Mitochondria were prepared (19) and Complex I isolated as described previously (20) using MS101 antibody from MitoSciences (Eugene, OR). The pH was adjusted to 6.8 for stepwise differential cysteine alkylation. The sample (~20 μl) was first treated with 10 μl of 10 mM perdeuterated *N*-ethylmaleimide (d_5-NEM), and excess reagent was then quenched with 3.6 μl of 30 mM cysteine. Oxidized cysteines were then reduced by the addition of 13 μl of DTT for 30 min, followed by alkylation with 18 μl of 100 mM d_0-NEM. All cysteine alkylation steps were performed at room temperature in the dark to minimize side reactions. The samples were then purified by SDS-PAGE using a 4–12% gradient gel (NuPAGE; Invitrogen). Detergent and other contaminants were removed by limiting electrophoretic travel (the sample was allowed to completely enter the top of the gel just below the loading well) to remove contaminants without separating the individual subunits of Complex I. The sample was then subjected to in-gel tryptic digestion as described previously (20).

Diamide Treatment—For some samples, following isolation of Complex I the sample was split, and one half was left untreated (control) and the other half oxidized by treatment with 150 μM diamide for 90 min at room temperature. Samples then underwent stepwise alkylation, purification, and tryptic digestion as described above. These samples served as a positive control for *in vivo* BSO-induced oxidation studies and to develop/validate a set of cysteine-specific multiple reaction monitoring (MRM) transitions used to quantitate reversible cysteine oxidations via MRM-mass spectrometry (MS).

Blue Native PAGE and in-Gel Complex I Activity Staining—Complex I activity following isolation as described above was confirmed in one control sample by blue native gel PAGE and then in gel Complex I activity using nitro blue tetrazolium assay as described by Ladha *et al.* (21). The sample was loaded onto a 4–12% gradient blue native gel PAGE 10 × cathode buffer (500 mM Tricine, 150 mM BisTris-HCl, 0.02% Coomassie Blue G-250, pH 7.0), 10 × anode buffer (500 mM BisTris-HCl, pH 7.0), 3 × gel buffer (150 mM BisTris, 1.5 M ϵ-aminocaproic acid, pH 7.0). In-gel Complex I activity determined by staining gel with buffer containing 2 mM Tris-HCl, pH 7.4, 0.1 mg/ml NADH and 2.5 mg/ml Nitro Blue tetrazolium at room temperature for 40 min.

Complex I Three-dimensional Imaging—The three-dimensional crystal structure of *Thermus thermophilus* Complex I solved by Efremov *et al.* (22) was used to view the local environments of specific cysteine residues in Complex I using the modeling program Chimera (University of California at San Francisco) and Protein Data Bank code 3M9S.

Mass Spectrometry—To identify relatively abundant Complex I peptides containing cysteine residues, isolated Complex I was subjected to in-gel protease digestion with trypsin and the resulting peptides analyzed by electrospray HPLC-MS/MS using a hybrid quadrupole time-of-flight mass spectrometer (QSTAR Elite, AB SCIEX) as described (20, 23). Chromatographic and MS method details have been reported previously (18, 24). All peptide assignments from the resulting MS data were made using the bioinformatics search engine Mascot version 2.2.04 (Matrix Sciences, London, UK) (25). The following search parameters were used: enzyme specificity was defined as trypsin, d_0-NEM and d_5-NEM fixed modifications were chosen. The variable modifications chosen were: acetyl (protein N terminus), Gln→pyro-Glu (N-terminal Gln), and oxidation (Met). The peptide ion (precursor) and the fragment ion mass tolerance were set at 0.2 and 0.4 Da for QSTAR data and 0.6 and 0.5 Da for QTRAP data, respectively. The maximum number of missed cleavages was set at 1 for tryptic digests. The publicly available SwissProt data base release version 57.12 containing 513,877 sequences and 180,750,753 residues was searched for data obtained from murine samples with species restriction *Mus musculus* (16,215 sequences). Ions scores are defined as [-10*Log(p)], where p is the probability that the observed match is a random event. Only peptide matches with an expectation score ≤0.05 were accepted. In cases where Mascot was unable to assign spectra to Complex I peptides, spectra were assigned manually using the following criteria: (i) the precursor and fragment ions must have good mass accuracy (<0.1 Da for QSTAR and <0.2 Da for QTRAP data), (ii) a *y*-fragment ion series is present that encompasses a minimum of three consecutive amino acids, (iii) only a limited number of unassigned ions are present, (iv) cysteine residues are present in their NEM alkylated state, and (v) fragment ions containing C-terminal proline residues must have a relative high abundance. Note, MS/MS spectra obtained from MRM-triggered enhanced product ion (EPI) scans were especially prone to yield low Mascot scores and required manually assignment.

To provide a quantitative comparison of the levels of cysteine oxidation, MRM-MS analysis targeted the levels of differentially alkylated (d_5 = reduced, d_0 = reversibly oxidized) cysteine-containing peptides. MRM precursor and fragment ion pair transitions were chosen based on the following guidelines: (i) no missed tryptic cleavage sites were present, (ii) peptides containing and single cysteine were preferred, (iii) for peptides containing two cysteine residues, the Q3 fragment ions was selected such that it contained only one cysteine to differentiate the oxidation status of each cysteine, (iv) the most intense *y* or *b* fragment ions were chosen for Q3, (v) *m/z* Q3 fragment ions were > *m/z* of the Q1 precursor, (vi) the data resulted in a single MRM peak with good chromatographic characteristics, and (vii) MRM transition and peptide identity were verified by MS/MS spectra via QSTAR analysis in IDA mode (abundant/easily ionized peptides) or QTRAP analysis by MRM-triggered EPI scans (low abundant peptides). For quantitation, a 4000 QTRAP hybrid triple quadrupole/linear ion trap mass spectrometer (AB SCIEX) was used as previously described (18, 24). Levels of cysteine oxidation were calculated as the percentage of the ion intensities of the reversibly oxidized peptide labeled with d_0-NEM for each condition (control, and BSO treated) over the sum of the reduced peptide labeled with d_5-NEM plus

TABLE 1

Murine Complex I protein coverage by LC-MS and number of Cys residues monitored per subunit

Mascot protein score and the total LC-MS sequence coverage obtained for all murine Complex I subunits are indicated as well as the total number of cysteine residues present in each subunit followed by the number of cysteines that were monitored for quantitation by MRM-MS experiments.

Subunit	Mascot protein score	LC-MS coverage	Total Cys in subunit	Cys monitored by MRM
		%		
Nd1	44	3	1	0
Nd2	33	7	1	0
Nd3	148	13	1	1
Nd4	219	10	3	0
Nd4L	NA[a]	0	2	0
Nd5	275	9	6	0
Nd6	NA	0	4	0
Ndufa1	220	30	1	0
Ndufa2	686	64	2	1
Ndufa3	131	61	0	0
Ndufa4	65	12	0	0
Ndufa5	592	64	1	1
Ndufa6	1,276	74	0	0
Ndufa7	1,333	86	1	1
Ndufa8	801	44	8	2
Ndufa9	768	42	2	2
Ndufa10	2,326	52	5	1
Ndufa11	NA	0	0	0
Ndufa12	1,098	80	1	1
Ndufa13	1,144	70	0	0
Ndufab1	163	21	5	0
Ndufb1	987	58	1	0
Ndufb2	65	9	1	0
Ndufb3	541	34	0	0
Ndufb4	605	70	0	0
Ndufb5	224	26	1	0
Ndufb6	521	58	0	0
Ndufb7	748	53	4	2
Ndufb8	730	38	1	0
Ndufb9	510	58	5	2
Ndufb10	987	58	5	1
Ndufb11	436	54	1	0
Ndufc1	NA	0	0	0
Ndufc2	619	67	1	0
Ndufs1	3,254	51	17	8
Ndufs2	1,988	48	7	2
Ndufs3	1,617	53	3	0
Ndufs4	809	62	1	0
Ndufs5	559	41	4	1
Ndufs6	732	68	3	1
Ndufs7	378	22	5	0
Ndufs8	1,092	30	8	2
Ndufv1	972	28	12	5
Ndufv2	507	41	6	0
Ndufv3	153	25	0	0
		Total	130	34

[a] NA, not applicable.

reversibly oxidized d_0-NEM-labeled peptide, *i.e.* (reversibly oxidized peptide d_0-NEM)/(reduced peptide d_5-NEM + reversibly oxidized peptide d_0-NEM) × 100. Fold change levels of reversibly oxidized cysteine peptides in BSO-treated were normalized to control levels; for each biological replicate (three total biological replicates), the percentage of reversibly oxidized cysteine peptides present for each experimental condition was divided by the percentage present in the control.

Statistical Analysis—Error bars represent S.D. from three biological replicates; three technical replicates were obtained for each sample; p values <0.05 were considered statistically significant. p values were quantified using Student's t test, two-tailed, equal variance.

RESULTS

Murine Complex I contains 130 cysteine residues distributed within 35 of its 45 total subunits (Table 1). Our goal in this study

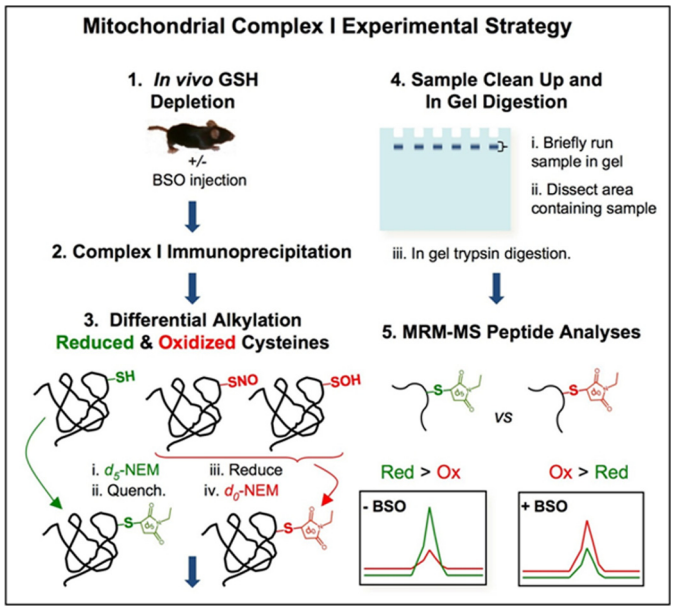

FIGURE 1. **Schematic diagram of experimental strategy.** Glutathione levels were depleted in the mouse brain via intraperitoneal BSO injection as described previously (7). Whole brain mitochondrial fractions were isolated and Complex I immunocaptured followed by stepwise differential alkylation. Briefly, reduced cysteine thiol groups (*green*) were initially labeled with d_5-NEM; excess d_0-NEM was then quenched with cysteine, followed by reduction of oxidized cysteines (*red*) with DTT. In the final step, formerly oxidized cysteines were alkylated with d_0-NEM. Although reversible cysteine modifications are represented in the figure as sulfenic acid (*SOH*) and *S*-nitrosylation (*SNO*), other reversible modifications could also occur that may undergo similar reactions, including intramolecular disulfide bonds and mixed disulfides with reduced or oxidized glutathione. Sample clean-up was achieved by briefly running NEM-labeled Complex I samples on SDS-polyacrylamide gels; samples were then dissected and subjected to in-gel tryptic digestion. Levels of cysteine oxidation were analyzed via MRM-MS as changes in the ratio of oxidized *versus* reduced peptide levels in control *versus* BSO-treated samples.

was to develop an approach that was capable of systematic mapping of the changes to reversible oxidation status of cysteines contained within Complex I subunits isolated from control *versus* glutathione-depleted mouse brains. Fig. 1 shows a schematic representation of the overall experimental strategy. Following three consecutive injections of BSO to deplete total glutathione to levels that mimic that within the PD brain (7), Complex I was isolated from whole brain (20) followed by stepwise differential alkylation with heavy deuterium-labeled d_5-NEM and d_0-NEM. These heavy and light NEM-labeled versions of the peptide represent reduced and reversibly oxidized versions of cysteine-containing peptides, respectively, and can be measured independently by MS analysis due to a 5-Da difference in their respective masses (18).

Our approach was specifically designed to purify the complex in its active and functional state in the shortest time possible under conditions that minimized any oxidation artifacts that might occur during isolation and workup. To achieve these goals, Complex I was first immunoprecipitated immediately after mitochondrial disruption according to a method we developed previously for its rapid isolation and purification (20). Second, the complex was alkylated prior to SDS-PAGE separation, as cysteine residues are especially prone to oxidation under these conditions (26, 27). In addition, all steps including differential alkylation were performed under conditions that maintain Complex I physically intact and at least in a partially func-

tionally active state, as determined by blue native gel electrophoresis and in-gel Complex I activity (nitro blue tetrazolium assay) (21) and shown in supplemental Fig. 42. It is also worth noting that we used the same antibody and immunoprecipitation procedure for Complex I as described in two previous studies (28, 29) that also reported that the flavin site of Complex I is still enzymatically active, therefore limiting susceptibility to nonspecific oxidation that might occur if the complex was dissociated or denatured.

To better quantify the reversible cysteine oxidation status of Complex I, we developed and validated 269 MRM precursor/fragment transitions representing 43 distinct cysteine residues within 17 subunits. Typically, this consisted of two to four transitions per peptide including d_0- and d_5-NEM-alkylated versions and methionine sulfoxide modifications (see supplemental Table 1, *A* and *B*). MRM transitions were generated by examining Mascot-assigned MS/MS spectra of Complex I peptides containing cysteine residues from previous MS-based proteomic experiments (20) and more recent LC-MS/MS analysis of isolated Complex I samples using a triple quadrupole instrument run in IDA mode. As described under "Experimental Procedures," MRM transitions were chosen based on several selection criteria that optimized for overall specificity and sensitivity, as well as ensuring that each precursor/fragment ion transition measures only one cysteine to differentiate oxidation status of each cysteine in peptides that contained more than one such residue. In our scheme, a quadrupole time-of-flight instrument (QSTAR Elite) was used for identifying peptides by MS/MS spectra due to its relatively high resolution and mass accuracy capabilities, whereas the hybrid triple quadrupole/linear ion trap instrument (4000 QTRAP) was best suited for identifying low abundant peptides due to its high sensitivity and targeting capabilities. Peptides for which it was difficult to obtain MS/MS spectra due to low abundance or low ionization efficiency were acquired by MRM-triggered EPI scans in the 4000 QTRAP. An example of such a triggered scan is presented in Fig. 2 where both MRM-MS and MS/MS data for the cysteine-containing peptide IIEQC^{347}LNK from the Ndufs1 subunit is shown. MS/MS peptide spectra annotated by Mascot as well as by manual assignment that contained one or more cysteines in Complex I and subsequently used for MRM assay development are provided as supplemental Figs. 1–40 which are indexed on supplemental Table 2.

Initial proof-of-principle experiments to demonstrate our ability to quantify changes in reversible cysteine oxidation were conducted using control *versus in vitro* diamide (150 μM, 90 min)-treated Complex I. Using a set of MRM transitions that represented 43 distinct cysteine-containing Complex I peptides, we were able to consistently monitor the reversible oxidation state of 34 cysteine residues; peptides containing methionine (Met) residues were monitored in the nonoxidized and sulfoxide states. On average, a 2.4-fold increase in cysteine oxidation was observed relative to controls in all cysteine-containing peptides (Fig. 3). The percentage of reversibly oxidized Complex I cysteines in control *versus* diamide-treated samples is depicted in supplemental Fig. 41 and supplemental Table 3. Compared with control samples, the diamide-treated samples were highly oxidized within a narrow range (74–93%, 85% average), likely indicating that maximum levels of diamide-mediated oxidation were attained for these cysteine residues and that most of the cysteines that were monitored were both solvent-accessible and reactive. Notably, control samples showed a wide range of cysteine oxidation (from 18–71%, 40% average). Cysteines that had a high level of oxidation in control samples and exhibited limited increases in oxidation due to diamide (Ndufa8–46, Ndufb7–59, and Ndufs1–564; see supplemental Fig. 41) may indicate cysteines with constitutive disulfide bonds. Alternatively, the ability of a cysteine thiol group to react with an alkylating reagent (d_0- or d_5-NEM) is dependent on both the redox state of the thiol group and its solvent accessibility. Because Complex I was not denatured under the differential alkylation procedure, limited solvent accessibility of a cysteine may influence the levels of oxidation measured. In this study our primary goal was to examine the sensitivity of Complex I cysteines to oxidative stress (specifically their reversible oxidation in an *in vitro* diamide-treated or *in vivo* glutathione depletion model) rather than focusing on the base-line levels of

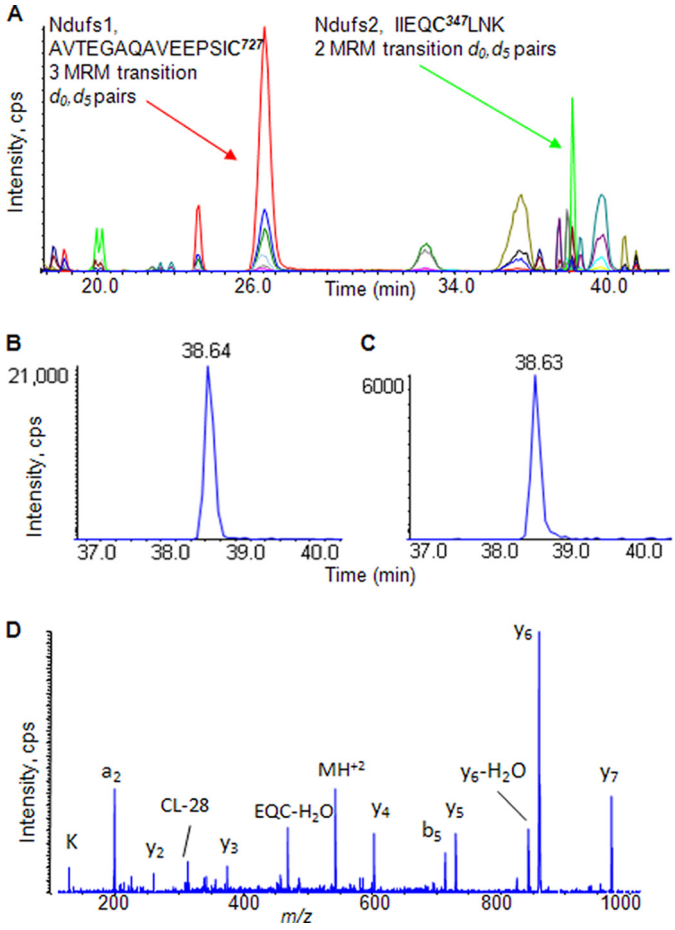

FIGURE 2. **MRM analysis and subsequent peptide identification.** *A*, total ion chromatograms of diamide-treated mouse brain Complex I examining 66 MRM transitions of 16 selected Cys-containing peptides with MRM transitions representing 2 different peptides. By following the ratio of peptide signals for diamide-treated samples using our differential alkylation strategy with d_0- and d_5-NEM, we can accurately quantify the reversible oxidation state of any specific cysteine residue at the peptide level. *B* and *C*, extracted ion chromatograms for oxidized (d_0) (*B*) and reduced (d_5) (*C*) NEM-labeled versions of the peptide IIEQC^{347}LNK from Complex I subunit Ndufs2. *D*, MS/MS spectra obtained by MRM-triggered EPI scan using the 4000 QTRAP identifies the peptide as IIEQCLNK. See supplemental Fig. 32 for spectra assignment.

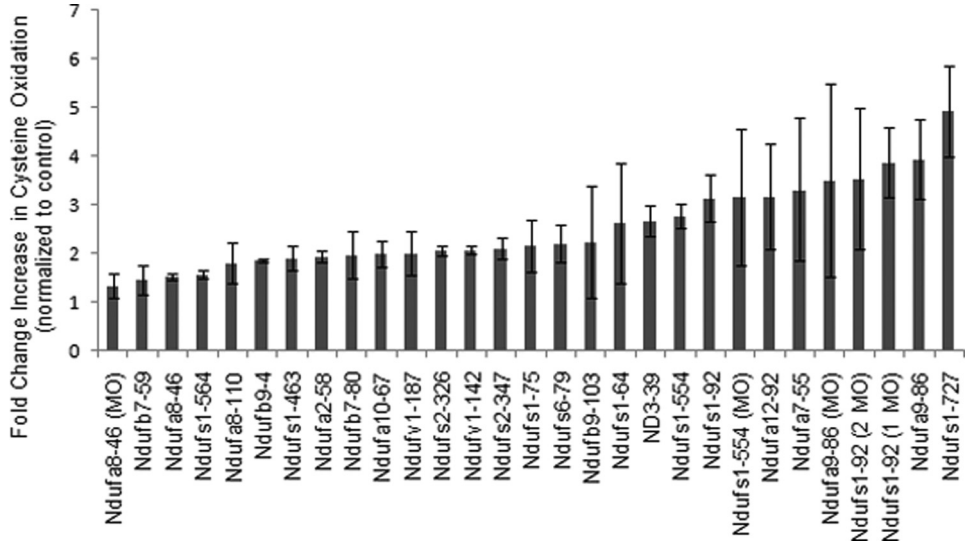

FIGURE 3. **Increased Complex I cysteine oxidation following *in vitro* treatment with diamide.** Complex I was isolated by immunocapture, half of the sample treated with 150 μM diamide for 90 min and the other half left untreated (control). Following treatment, samples were differentially alkylated with d_5- and d_0-NEM and analyzed by MRM-MS. Data are presented as–fold change increase in Complex I cysteine oxidation relative to control levels. Cysteine-containing peptides (*x* axis) are represented by gene name for the Complex I subunit followed by the cysteine residue number (protein sequence from Uniprot). *MO*, methionine sulfoxide. Peptide identities and statistics are presented in supplemental Table 3. *Error bars* represent the S.D. of three biological replicates; three technical replicates were obtained for each sample.

cysteine oxidation itself. Changes in the level of oxidation will be reflected by a difference in the ratio of d_0- to d_5-NEM-labeled peptides independent of base-line levels of oxidation, therefore these results focus on the sensitivity of specific cysteines to oxidation.

Next, we employed this set of validated MRM transitions developed from diamide-treated reversible cysteine oxidation to Complex I samples isolated from the brains of untreated and BSO-treated mice that had both undergone differential alkylation with d_0- and d_5-dialmide (see Fig. 1). In total, we were able to monitor the percentage of reversible cysteine oxidation in 34 distinct cysteines from control and BSO-treated murine Complex I brain samples. However, only six peptides were identified from three separate subunits (Ndufs1 = VVAAC^{92}AMPVMK, HSFC^{463}EVLK, MLFLLGADGGC^{554}ITR; Ndufs2 = IIEQC^{347}LNK; and Ndufb7 = DYC^{59}AHYLIR, DSFPNFLAC^{80}K; numbers indicate the sequence position of cysteines within the particular Complex 1 subunit) that showed statistically increased oxidation compared with untreated mouse brain controls as a consequence of BSO-mediated glutathione depletion (Fig. 4). No significant change in oxidation was detected in the other 28 cysteine residues monitored by MRM (see supplemental Table 4). To verify peptide identities following MRM analysis, an aliquot of control and BSO-treated samples were separately analyzed by LC-MS/MS analysis on the QSTAR platform.

To provide information on the local environment and solvent accessibility of the six statistically relevant oxidized cysteines in glutathione-depleted brains (Fig. 4), the corresponding amino acids of Complex I from *T. thermophilus* have been identified in Table 2. The location of these residues on the entire protein complex and the quarternary structure is presented (Fig. 5, *A* and *B*) using the three-dimensional crystal structure of *T. thermophilus* Complex I solved by Efremov *et al.* (22). An enlarged view of Nqo4-Ala^{293} (Fig. 5*C*) reveals the orientation of this residue toward the center of the complex as part of an alpha-helix, whereas Nqo3-Cys^{83} (Fig. 5*D*) is associated with an iron-sulfur complex, suggesting that these residues would be more resistant to oxidation. However, two of the *T. thermophilus* amino acids (Nqo3-Val^{571} Fig. 5*E* and Nqo3-Lys^{494} Fig. 5*F*), which correspond to murine Complex I cysteines, are potentially in solvent-exposed environments, indicative of residues that may have increased sensitivity to oxidation as observed in our results. Data obtained from mammalian mitochondrial Complex I in the future may explain these discrepancies of oxidant sensitivity.

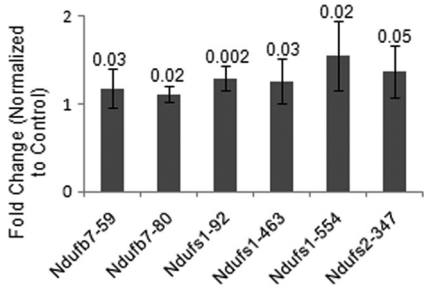

FIGURE 4. **Increased cysteine oxidation of mouse brain Complex I subunits as a consequence of glutathione depletion.** Reversible cysteine oxidation of Complex I peptides were measured by MRM-MS in mouse brain samples following *in vivo* glutathione depletion. Six cysteine-containing peptides from three Complex I subunits with increased oxidation were identified. Cysteine-containing peptides are represented by gene name for the Complex I subunit followed by the cysteine residue number (protein sequence from Uniprot). Significance was determined by *p* values <0.05 (posted above *error bars*) as quantified using a Student's *t* test, two-tailed, equal variance. *Error bars* represent the S.D. of three biological replicates, three technical replicates for each sample. *Numbers* associated with each subunit (*x* axis) indicate the position of the cysteine residue in the protein sequence. See supplemental Table 2 for peptide identities.

DISCUSSION

Using differential alkylation of cysteine residues by d_0- and d_5-NEM, we were able to monitor the reversible oxidation

TABLE 2

***T. thermophilus* amino acids that correspond to murine Complex I cysteines based on sequence homology**

Mouse Complex I subunit-Cysteine	Corresponding *T. thermophilus* subunit-amino acid	Mouse sequence containing Cys of interest	Corresponding *T. thermophilus* sequence
Ndufs1-Cys^{92}	Nqo3-Cys^{83}	PKVVAAC^{92}AMPVMK	PKLAASC^{83}VTAVAD
Ndufs1-Cys^{463}	Nqo3-Lys^{494}	—-SFC^{463}EVLKDA	EMVAKAK^{494}EAWEKA
Ndufs1-Cys^{554}	Nqo3-Val^{571}	LGADGGC^{554}ITRQDL	-AYYGFV^{571}PPEEAL
Ndufs2-Cys^{347}	Nqo4-Ala^{293}	RIIEQC^{347}LNKMPP	KIIKQA^{293}LERLEP

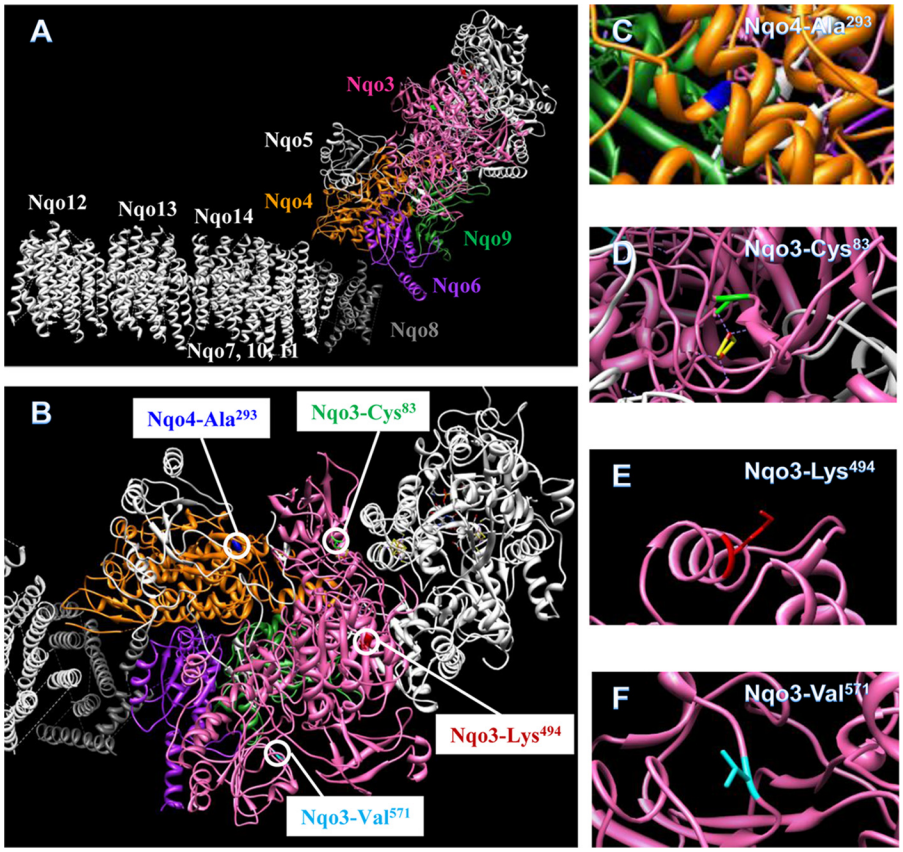

FIGURE 5. **Three-dimensional environment of *T. thermophilus* Complex I amino acids that correspond to murine Complex I cysteines with increased oxidation due to GSH depletion.** The three-dimensional crystal structure of *T. thermophilus* Complex I solved by Efremov *et al.* (22) was used to identify the local environment of Complex I amino acids using the modeling program Chimera and Protein Data Bank code 3M9S. *A*, side view of the entire *T. thermophilus* Complex I three-dimensional structure. Subunits that correspond to murine Complex I subunits of interest are *color coded* and indicated on Table 2. Note some Complex I subunits that are not relevant for this study are left unlabeled. *B*, top view of the hydrophilic arm of *T. thermophilus* Complex. The locations of the four amino acids corresponding to murine Complex I cysteines listed on Table 2 are indicated. *C–F*, local environments of *T. thermophilus* Complex I amino acids. Nqo4-Ala^{293} (*blue*) is part of an α-helix and is oriented toward the inside of the complex (*C*). Nqo3-Cys^{83} (*green*) is shown as part of an iron-sulfur cluster (*yellow square* with *red corners*) and appears to be only partially exposed to the environment (*D*). Nqo3-Lys^{494} (*red*) shown extending into the environment as part of an exposed α-helix (*E*). Nqo3-Val^{571} (*teal*) is an exposed amino acid on the surface of the complex (*F*).

states of 34 distinct cysteine residues contained within 17 Complex I subunits isolated from control *versus* glutathione-depleted mouse brains, a physiologically relevant oxidative stress model for PD. This redox analysis was accomplished in our laboratory by adapting a recent strategy developed called OxMRM (18) to quantify site-specific cysteine oxidation within protein complexes. This method incorporates rapid and highly efficient isolation of Complex I, stepwise thiol-specific differential alkylation with d_0- and d_5-NEM to label reduced *versus* oxidized cysteine-containing residues, and finally, sensitive quantitation by targeted MRM assays after labeling and proteolytic digestion. MRM-MS is a robust and sensitive quantitative approach (30, 31) shown to have a wide dynamic range for peptide detection and quantitation up to 5–6 orders of magnitude (32–34). In this strategy, it was used for the detection of even low abundance protein alterations in a reproducible and flexible manner. Overall, this strategy identified six cysteine-containing peptides with significantly increased reversible oxidation as a result of glutathione depletion, three of which were found within subunits containing iron-sulfur clusters essential for electron transport.

It has been demonstrated previously that the Ndufs1 subunit of Complex I is sensitive to cysteine oxidation via *S*-nitrosylation, resulting in decreased Complex I activity (17). However, few published reports have attempted to quantify Complex I cysteine oxidation. Sethuraman *et al.* (35) used a proteomic approach utilizing isotope-coded affinity tagged proteins for MS analysis from rabbit heart tissue. This study and our data both observe that a cysteine-containing peptide, TTGLVGLAVC^{17}DTPHER from subunit Ndufa5 is sensitive to exogenous sources of oxidation such as diamide treatment; however, we observed no significant change in oxidation in glu-

tathione-depleted mouse brains. Another study reported a selective glutathionylation of Cys-554 from the Ndufs1 subunit in bovine heart following elevated oxidative stress (16). This cysteine was also found to be significantly oxidized (~1.5-fold increase relative to control; Fig. 4) in our study. The location of the corresponding *T. thermophilus* amino acids to these oxidized cysteines (Fig. 5 and Table 2) were found to be located near more solvent-accessible sites, which may in part explain the increased sensitivity of these cysteines to oxidation. In this report, all peptides were numbered based on intact protein sequences from Uniprot, whereas other publications may assign sequence protein numbers after mitochondrial targeting sequences have been cleaved (*e.g.* Cys-554 in this paper corresponds to Cys-531 in Ref. 16).

Although the precise three-dimensional structure of mammalian Complex I remains unsolved, the crystal structure of the hydrophilic domain of a bacterial (*T. thermophilus*) analog of Complex I has been reported (36) and more recently, the complete structure of Complex I from *T. thermophilus* (22). The hydrophilic domain of *T. thermophilus* Complex I analog is composed of 7 subunits (Nqo1–6 and Nqo9) and contains the NADH binding site along with redox components such as the flavin mononucleotide (FMN) and electron-transporting iron-sulfur clusters. These structural data have allowed for the functional assignment of many cysteine residues including those that are part of iron-sulfur clusters (36, 37). To gain functional insight into the mammalian Complex I cysteines that we identified under conditions of glutathione-induced oxidation, the protein sequences of mammalian Complex I subunits were aligned using the Basic Local Alignment Search Tool (Blast) to the *T. thermophilus* proteome. Subunits Nqo3 and Nqo4 correspond to mammalian Complex I subunits Ndufs1 and Ndufs2, respectively, whereas Ndufb7 has no *thermophilus* analog. Blast alignment of murine Ndufs1and Ndufs2 (Uniprot ID Q91VD9 and Q91WD5, respectively) against *T. thermophilus* Nqo3 and Nqo4 subunits is shown in supplemental Figs. 43 and 44. Analysis of this Blast alignment demonstrates that Cys-463 and Cys-554 of Ndufs1 do not correspond to any cysteines present on Nqo3 and may exist as a disulfide bond or could function through an unknown mechanism. Evidence from the three-dimensional structure of *T. thermophilus* Complex I suggests that the corresponding amino acids to Cys-554 and Cys-463 of Ndufs1 (Fig. 5, *E* and *F*) may exist on the surface of the complex in a solvent-exposed state, which may result in its observed susceptibility to oxidation. Cys-347 of Ndufs2 is surrounded by several other cysteines in an orientation suggestive of an iron-sulfur consensus sequence (indicated by Uniprot Q91WD5), although currently no experimental data support this, and no corresponding cysteine residue exists in Nqo4. Cys-92 of Ndufs1 corresponds with Cys-83 of Nqo3 which is part of an 2Fe-2S iron-sulfur cluster designated N1b (36). Oxidation of Cys-92 within Ndufs1 could conceivably directly impair electron transport and disrupt Complex I activity. Because Complex I activity is an integral component for maintaining proper mitochondrial membrane potential and ultimately producing ATP which is critical for maintaining proper mitochondrial function, even a partial disruption in Complex I activity may stress already susceptible dopaminergic midbrain neurons (4–6).

Our results represent an intermediate step toward a complete mapping of cysteine oxidation within Complex I, allowing monitoring of 34 of the 130 total cysteines. By adapting a previously established method (18) developed in our laboratory for targeting the oxidation states of cysteines in a single targeted protein for use in a large multiprotein complex, we have demonstrated the effectiveness of this strategy to quantify the oxidation of multiple cysteines of Complex I in a single experiment and will be valuable for future studies of cysteine oxidation. Complex I isolation efficiency was found sufficient enough to obtain an average protein coverage for each subunit by LC-MS of ~40% (Table 1), which includes four problematic subunits with no coverage. Additionally, the mitochondrial-encoded subunits Nd1–Nd6 displayed low overall LC-MS protein coverage compared with nuclear-encoded subunits, which limited our ability to quantify cysteine-containing peptides from these relatively hydrophobic subunits. Tryptic digestion of Complex I often resulted in peptides that were not amenable to identification by LC-MS; however, due to this effective isolation and analysis scheme, we predict that we should be able to significantly increase the number of cysteine-containing Complex I peptides that we can monitor by MRM if additional proteases are employed. Because our strategy uses DTT treatment for the reversible conversion of oxidized cysteines to reduced cysteines, the expectation is that all solvent-accessible oxidized cysteines with the exception of sulfinic and sulfonic acids (Cys-SO_2H and Cys-SO_3), including *S*-nitrosylation, glutathionylation, disulfides, and sulfenic acid (Cys-SOH), will be labeled by differential sulfhydryl-specific NEM alkylation. Moreover, reversibility in this context does not imply that DTT-reduced Complex I is identical to the state prior to oxidation as both oxidized cysteines that are solvent inaccessible and DTT-irreversible modifications (*i.e.* sulfinic and sulfonic acids) would at minimum be unchanged.

Further method development could, in principle, also allow expansion of our analysis to include irreversible cysteine oxidative modifications such as sulfinic and sulfonic acid. In such a scheme, one would need to target specifically these nonreversibly oxidized cysteine-containing peptides that were not amenable to NEM alkylation, possibly by employing synthetic heavy isotope-labeled peptide analogs as standards. Future site-directed mutagenesis studies on cysteines sensitive to oxidative stress should in principle allow us also to determine the potential causative effects of these specific alterations on Complex I activity. The identification of several cysteine residues in Complex I that have vital functions (such as electron transport) that are also sensitive to endogenous oxidative stress may provide valuable insight into the association or causation of Complex I dysfunction in diseases like PD.

REFERENCES

1. Nicklas, W. J., Vyas, I., and Heikkila, R. E. (1985) *Life Sci.* **36,** 2503–2508
2. Heikkila, R. E., Nicklas, W. J., Vyas, I., and Duvoisin, R. C. (1985) *Neurosci. Lett.* **62,** 389–394
3. Schapira, A. H., Cooper, J. M., Dexter, D., Jenner, P., Clark, J. B., and Marsden, C. D. (1989) *Lancet* **1,** 1269
4. Perry, T. L., Godin, D. V., and Hansen, S. (1982) *Neurosci. Lett.* **33,**

305–310
5. Perry, T. L., and Yong, V. W. (1986) *Neurosci. Lett.* **67,** 269–274
6. Jenner, P. (1993) *Acta Neurol. Scand. Suppl.* **146,** 6–13
7. Andersen, J. K., Mo, J. Q., Hom, D. G., Lee, F. Y., Harnish, P., Hamill, R. W., and McNeill, T. H. (1996) *J. Neurochem.* **67,** 2164–2171
8. Chinta, S. J., and Andersen, J. K. (2006) *Free Radic. Biol. Med.* **41,** 1442–1448
9. Jha, N., Jurma, O., Lalli, G., Liu, Y., Pettus, E. H., Greenamyre, J. T., Liu, R. M., Forman, H. J., and Andersen, J. K. (2000) *J. Biol. Chem.* **275,** 26096–26101
10. Hsu, M., Srinivas, B., Kumar, J., Subramanian, R., and Andersen, J. (2005) *J. Neurochem.* **92,** 1091–1103
11. Chinta, S. J., Kumar, J. M., Zhang, H., Forman, H. J., and Andersen, J. K. (2006) *Free Radic. Biol. Med.* **40,** 1557–1563
12. Chinta, S. J., Kumar, M. J., Hsu, M., Rajagopalan, S., Kaur, D., Rane, A., Nicholls, D. G., Choi, J., and Andersen, J. K. (2007) *J. Neurosci.* **27,** 13997–14006
13. Giles, N. M., Watts, A. B., Giles, G. I., Fry, F. H., Littlechild, J. A., and Jacob, C. (2003) *Chem. Biol.* **10,** 677–693
14. Schilling, B., Yoo, C. B., Collins, C., and Gibson, B. W. (2004) *Int. J. Mass Spectrom.* **236,** 117–127
15. Di Simplicio, P., Franconi, F., Frosalí, S., and Di Giuseppe, D. (2003) *Amino Acids* **25,** 323–339
16. Hurd, T. R., Requejo, R., Filipovska, A., Brown, S., Prime, T. A., Robinson, A. J., Fearnley, I. M., and Murphy, M. P. (2008) *J. Biol. Chem.* **283,** 24801–24815
17. Burwell, L. S., Nadtochiy, S. M., Tompkins, A. J., Young, S., and Brookes, P. S. (2006) *Biochem. J.* **394,** 627–634
18. Held, J. M., Danielson, S. R., Behring, J. B., Atsriku, C., Britton, D. J., Puckett, R. L., Schilling, B., Campisi, J., Benz, C. C., and Gibson, B. W. (2010) *Mol. Cell. Proteomics* **9,** 1400–1410
19. Trounce, I. A., Kim, Y. L., Jun, A. S., and Wallace, D. C. (1996) *Methods Enzymol.* **264,** 484–509
20. Schilling, B., Bharath, M. M. S., Row, R. H., Murray, J., Cusack, M. P., Capaldi, R. A., Freed, C. R., Prasad, K. N., Andersen, J. K., and Gibson, B. W. (2005) *Mol. Cell. Proteomics* **4,** 84–96
21. Ladha, J. S., Tripathy, M. K., and Mitra, D. (2005) *Cell Death Differ.* **12,** 1417–1428
22. Efremov, R. G., Baradaran, R., and Sazanov, L. A. (2010) *Nature* **465,** 441–445
23. Schilling, B., Murray, J., Yoo, C. B., Row, R. H., Cusack, M. P., Capaldi, R. A., and Gibson, B. W. (2006) *Biochim. Biophys. Acta* **1762,** 213–222
24. Danielson, S. R., Held, J. M., Schilling, B., Oo, M., Gibson, B. W., and Andersen, J. K. (2009) *Anal. Chem.* **81,** 7823–7828
25. Perkins, D. N., Pappin, D. J., Creasy, D. M., and Cottrell, J. S. (1999) *Electrophoresis* **20,** 3551–3567
26. Taylor, F. R., Prentice, H. L., Garber, E. A., Fajardo, H. A., Vasilyeva, E., and Blake Pepinsky, R. (2006) *Anal. Biochem.* **353,** 204–208
27. Perdivara, I., Deterding, L. J., Przybylski, M., and Tomer, K. B. (2010) *J. Am. Soc. Mass. Spectrom.* **21,** 1114–1117
28. Nadanaciva, S., Dykens, J. A., Bernal, A., Capaldi, R. A., and Will, Y. (2007) *Toxicol. Appl. Pharmacol.* **223,** 277–287
29. Willis, J. H., Capaldi, R. A., Huigsloot, M., Rodenburg, R. J., Smeitink, J., and Marusich, M. F. (2009) *Biochim. Biophys. Acta* **1787,** 533–538
30. Tiller, P. R., Cunniff, J., Land, A. P., Schwartz, J., Jardine, I., Wakefield, M., Lopez, L., Newton, J. F., Burton, R. D., Folk, B. M., Buhrman, D. L., Price, P., and Wu, D. (1997) *J. Chromatogr. A* **771,** 119–125
31. Lee, M. S., and Kerns, E. H. (1999) *Mass Spectrom. Rev.* **18,** 187–279
32. Anderson, L., and Hunter, C. L. (2006) *Mol. Cell. Proteomics* **5,** 573–588
33. Keshishian, H., Addona, T., Burgess, M., Kuhn, E., and Carr, S. A. (2007) *Mol. Cell. Proteomics* **6,** 2212–2229
34. Picotti, P., Bodenmiller, B., Mueller, L. N., Domon, B., and Aebersold, R. (2009) *Cell* **138,** 795–806
35. Sethuraman, M., McComb, M. E., Huang, H., Huang, S., Heibeck, T., Costello, C. E., and Cohen, R. A. (2004) *J. Proteome Res.* **3,** 1228–1233
36. Sazanov, L. A., and Hinchliffe, P. (2006) *Science* **311,** 1430–1436
37. Hinchliffe, P., and Sazanov, L. A. (2005) *Science* **309,** 771–774